A 1-D Vaneless Diffuser Model Accounting for the Effects of Spanwise Flow Stratification

A 1-D Vaneless Diffuser Model Accounting for the Effects of Spanwise Flow Stratification

Charles Stuart[1], Stephen Spence[1], Sung In Kim[1], Dietmar Filsinger[2] & Andre Starke[2]

[1] School of Mechanical and Aerospace Engineering, Queen's University Belfast
Ashby Building, Stranmillis Road, Belfast, BT9 5AH
[2] IHI Charging Systems International GmbH

ABSTRACT

The radial vaneless diffuser, though comparatively simple in terms of geometry, poses a significant challenge in obtaining an accurate 1-D based performance prediction due to the swirling, unsteady and distorted nature of the flow field. Turbocharger compressors specifically, with the ever increasing focus on achieving a wide operating range, have been recognised to operate with significant regions of spanwise separated flow, particularly at off design conditions.

Using a combination of single passage Computational Fluid Dynamics (CFD) simulations and extensive gas stand test data for three geometries, the current study aims to evaluate the onset and impact of spanwise flow stratification in radial vaneless diffusers, and how the extent of the aerodynamic blockage presented to the flow throughout the diffuser varies with both geometry and operating condition. Having analysed the governing performance parameters and flow phenomena, a novel 1-D modelling method is presented and compared to an existing baseline method as well as test data to quantify the improvement in prediction accuracy achieved.

NOMENCLATURE

A	Flow area (m^2)
AR	Area Ratio of diffuser (-)
b	Passage height (m)
B	Blockage (-)
C_f	Skin friction coefficient (-)
CP	Static pressure recovery coefficient (-)
D	Diameter (m)
I	Ideal / Isentropic
k	Skin friction constant (-)
$\dot{m}$	Mass flow rate (kg/s)
p	Static pressure (Pa)
p_0	Total pressure (Pa)
PR	Total-total pressure ratio (-)
r	Radius (m)
R	Gas constant (J/kgK)
Re	Reynolds number (-)
RR	Radius Ratio of diffuser (-)
T	Temperature (K)
T_0	Total temperature (K)
U	Blade speed (m/s)
V	Absolute velocity (m/s)
$\dot{V}$	Volumetric flow rate (m^3/s)
Y_D	Diffuser loss coefficient (-)
α_2	Mean impeller tip flow angle relative to radial (°)
β	Flow angle relative to meridional (deg)
γ	Ratio of specific heats (-)
η	Isentropic total-total efficiency (-)
ρ	Density (kg/m^3)
ϕ	Local flow coefficient (-)
ϛ	Diffuser inlet flow parameter (-) $\left[\varsigma = \frac{\dot{V}\sqrt{\gamma R T_{01}}}{U_2{}^2 D_2{}^2}\right]$
1-D	One-dimensional
SFM	Swirl flow meter
VLD	Vaneless diffuser

Subscripts:

i	Calculation step
I	Ideal
r	Radial direction
TT	Total –to-total
u	Tangential direction
1	Stage inlet
2	Impeller exit / vaneless diffuser inlet
3	Vaneless diffuser exit
4	Volute exit measurement plane
max	Maximum value for a given parameter

INTRODUCTION

The radial vaneless diffuser, though comparatively simple in terms of geometry, poses a significant challenge in obtaining an accurate 1-D performance prediction due to the highly swirling, distorted and unsteady nature of the flow field emanating from the impeller. The distorted nature of the flow has constituents in both the pitchwise and spanwise directions, arising from the characteristic jet-wake impeller exit flow field and the curvature of the shroud wall respectively. Clearly, accounting for these flow features is of paramount importance if a clear indication of performance is to be obtained, particularly at off-design conditions.

It is of course recognised that while the computational capability exists to complete full stage three dimensional (3-D) CFD simulations in order to design centrifugal compressors, this approach must still be complemented by a well validated 1-D tool to perform an initial design optimisation, thus helping to minimise the overall time to market. With the increasing implementation of engine downsizing technologies in all of the major world markets, this is clearly a significant consideration for turbocharger manufacturers in particular. Furthermore, 1-D modelling can still prove to be a useful tool for generating a deeper understanding of centrifugal compressor aerodynamics, provided it works to account for each source of loss within the stage individually. By fundamentally evaluating the flow phenomena contributing to

ISBN978-4-89111-008-6

entropy generation across the entire operating range, and capturing the associated performance decrement on a 1-D basis, timely feedback can be provided to the designer to identify the major sources of loss within the stage, ultimately allowing corrective action to be taken. However, while existing 1-D centrifugal compressor design techniques have a proven ability to accurately predict performance near the best efficiency point, it is off-design conditions which are of the greatest interest for turbocharging applications and where further improvement in the existing modelling methods is required.

A recent focus on the characterisation of impeller recirculation by Harley *et al*. [1] demonstrated the propensity of modern automotive turbochargers to operate with significant regions of recirculation at the inlet, leading to, among other impacts, significant regions of aerodynamic blockage being presented to the incoming flow. Impeller exit recirculation too has received some attention in recent years, with Qiu *et al.* [2] providing a means of characterising the recirculation present in the blade to blade plane. As is frequently the case with centrifugal compressor aerodynamics, the impeller has led the way. The current work however aims to redress the balance and evaluate the impact of flow separation and recirculation and the associated spanwise aerodynamic blockage provided to the flow in radial vaneless diffusers.

The meridional curvature in the hub to shroud plane and the blade passage curvature result in the flow being stabilised at the suction and shroud side corner of the impeller passage, creating a sink for low energy particles, encouraging boundary layer growth and separation. By comparison, at the pressure and hub side of the passage there is an accumulation of high energy particles, increasing the free stream velocity and hence reducing separation tendencies. It is this flow stratification effect which the current work is attempting to account for, by considering the impact of the low energy region as providing an aerodynamic blockage to the flow field in the spanwise direction.

Previous work by the authors [3] relating to an evaluation of existing 1-D vaneless diffuser modelling methods for turbocharger centrifugal compressor applications highlighted the importance of accounting for the presence of spanwise aerodynamic blockage at the entrance to the diffuser when specifying the flow field. An approach involving the use of single passage CFD simulations for each of the compressor stages in question was utilised to permit a correlation capturing the influence of geometry and operating condition to be generated. A new diffuser inlet flow parameter, as depicted in Eq. (1), also had to be specified in order to allow the variation of diffuser inlet blockage with both geometry and operating condition to be captured within a representative non-dimensional parameter that could be applied to any data set. The resulting flow parameter, which captures the dominant diffuser inlet flow variables identified by Cumpsty [4] equates to the quotient of local flow coefficient and impeller tip Mach number, henceforth represented by ϟ.

$$ϟ = \frac{\dot{V}\sqrt{\gamma R T_{01}}}{{U_2}^2 {D_2}^2} \quad (1)$$

The resulting empirical relationship between diffuser inlet blockage B_2 and the diffuser inlet flow parameter ϟ amounted to a quartic fit line, as shown by Eq. (2).

$$B_2 = 91900ϟ^4 - 62100ϟ^3 + 15500ϟ^2 - 1730ϟ + 90.6 \quad (2)$$

The characterisation work pertaining to diffuser inlet aerodynamic blockage demonstrated the presence of significant levels of blockage (up to 60%), particularly towards the surge side of the map. Specification of this parameter permitted the complete flow field at inlet to the diffuser to be specified from gas stand test data, allowing an evaluation of different existing meanline diffuser modelling methods to be undertaken.

The resulting modelling evaluation highlighted that the use of an equivalent skin friction coefficient (C_f) as a bulk loss term in 1-D diffuser modelling can, when tuned correctly, deliver a performance prediction within an acceptable window of accuracy. However, such a method does not permit the designer to interrogate the results from the model and easily identify the predominant sources of loss, making it of limited use as a design tool.

The natural progression from this work, which demonstrated the limitations in existing methods, was to extend the findings in terms of aerodynamic blockage levels at the inlet of the diffuser to define a new modelling method. The meanline modelling approach attributed to the vaneless diffuser differs somewhat to that utilised in the performance prediction of the other stage elements , where it is usually assumed that the flow completely fills the passages and passes from one measurement point to the next isentropically, with empirical losses applied at the interfaces. By comparison, 1-D vaneless diffuser modelling methods have effectively ubiquitously utilised a calculation method involving calculating flow conditions at a number of discrete radial steps throughout the diffuser, as outlined in the work of Stanitz [5] and Herbert [6]. As a result of this, it is necessary to know not only how the levels of blockage at diffuser inlet vary with geometry and operating condition, but also how this varies throughout the radial extent of the diffuser.

It is also worth acknowledging the rigorous contribution made by Dubitsky and Japikse [7] in developing a two-zone diffuser model and connecting it to a two-zone impeller model. However, as the ultimate aim of the current work is the improvement in the performance prediction delivered by a single-zone model, the above approach is not applicable.

The current work focuses on quantifying the degree of spanwise separation of the flow, and how this is related to geometry and operating condition. While it would be ideal to directly evaluate the extent of the resulting aerodynamic blockage presented to the flow from test data, the scale of the stages being investigated does not permit the necessary instrumentation to be reasonably incorporated. The alternative approach applied for the current study was the use of single passage CFD simulations for each geometry; the validation of each against gas stand test data is presented in a subsequent section.

Comparisons based on the resulting performance prediction were drawn between the proposed modelling method, the baseline Herbert vaneless diffuser model and gas stand test data. Three modern automotive turbocharger centrifugal compressors, denoted C-4, C-5 and C-6 respectively, were used in this investigation. All three compressors possessed unshrouded impellers, utilized vaneless diffusers and backswept impeller blading, indications to the dimensions of which are depicted in Table 1. It is worth emphasising that all three geometries are typical of automotive stages, being devoid of recirculating casing treatments and pre-swirl vanes. The baseline geometry (C-4) was designed for an automotive gasoline engine of 2.0L swept volume.

Table 1: Tested compressor stage geometries

	ΔD_2 (%)	Δb_2 (%)	$\Delta(D_3/D_2)$ (%)
C-4	-	-	-
C-5	+30.8	+24.3	-8.33
C-6	+48.7	+25.1	-6.81

MODELLING

The modelling work undertaken for the current study comes under two headings. Firstly, single passage CFD simulations to allow the blocked region to be evaluated and the impact on the flow field to be determined. Secondly, 1-D radial diffuser modelling, illustrating how the findings from the CFD study were implemented into a new modelling method.

CFD Methodology

The chosen package for conducting all CFD simulations

within the current work was ANSYS CFX14.0. In order to balance the requirements for calculation time and modelling accuracy, the approach taken was to employ single passage simulations rather than a full stage calculation. While this neglects the presence of the scroll volute as is effectively universally found on turbocharger compressors, it will be shown that when coupled with the correct post processing techniques, the results from the single passage simulations will demonstrate a satisfactory degree of accuracy.

The modelling configuration applied for each of the compressors followed that as described by Harley *et al.* [1], as illustrated in Figure 1. The single passage model was defined to contain three separate domains, two stationary domains for the inlet and diffuser respectively, and one rotating domain for the impeller. In each case, frozen rotor interfaces were used to connect the stationary and rotating domains. In order to include the influence of tip clearance flows on the simulation results, 30 cells were placed in the blade tip gaps and a counter rotating velocity was applied to the impeller shroud wall to render it effectively stationary.

As shown in Figure 1, the total cell count was approximately 1.6 million, a value arrived at through having conducted a grid independence study. The Shear Stress Transport (SST) turbulence model was employed, necessitating y+ to be maintained below five in all three domains, with a level of less than two being achieved throughout the majority of the model. The measurement planes (MP) depicted in Figure 1 correspond with those available from test data and with 1-D interstage measurement points.

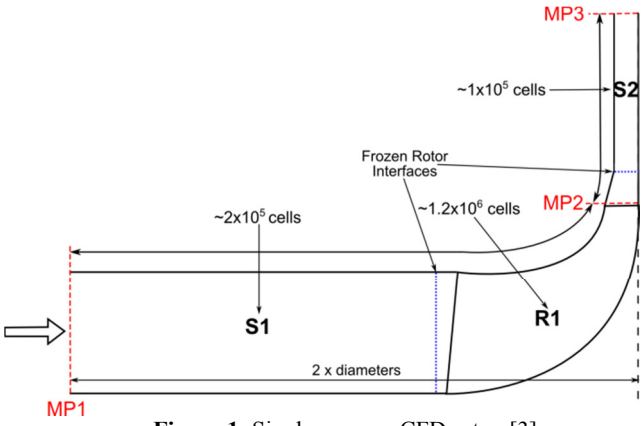

Figure 1: Single passage CFD setup [3]

In terms of solver convergence criteria, convergence was deemed to have been achieved when the RMS residuals fell below $1x10^{-4}$ [8], the imbalances of mass, energy and momentum across the model fell below 0.01%, and the total-to-total isentropic efficiency fluctuations were less than 0.05%. Surge was defined when the solver failed to meet the convergence criteria.

In order to better replicate the real compressor stage, additional loss terms had to be applied to account for aspects not represented within the single passage models. During the post processing of the CFD data two additional 1-D losses were applied, namely the volute loss model of Weber and Koronowski [9], and the disk friction loss of Whitfield [10]. The resulting CFD predictions are compared with test data in the next section.

CFD Validation

In order to establish confidence in the accuracy of the CFD predictions, the CFD predicted compressor maps of both total pressure ratio and total-to-total isentropic efficiency were compared to those gathered during gas stand testing in QUB. The layout of the test facility is depicted schematically in Figure 2.

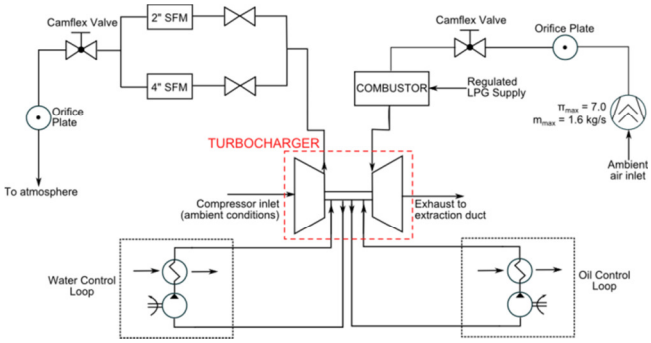

Figure 2: Schematic of QUB turbocharger test facility

The entirety of the test data was gathered in accordance with SAE J1826 [11] for two-loop hot gas test stands. Mass flow measurements were collected using one of the two ABB FS4000-ST4 swirl flow meters depicted in Figure 2, to an error of less than ±0.5% at reference flow conditions [17]. Compressor rotational speed was measured using an eddy current based sensor to pick up the impeller blade passing frequency. Static pressure data was gathered using Druck PMP 4000 Series gauge pressure transducers, delivering readings to an accuracy of ±0.04% full scale [18]. Temperature measurements on the compressor side of the rig, as well as at turbine discharge, were logged using calibrated BS1904 [12] Class-A PT-100 resistance thermometers. By comparison, turbine inlet temperatures were gathered using K-type thermocouples. During data post processing, in order to obtain a pressure or temperature value at a particular position, the arithmetic mean of the numerous circumferential values was calculated in order to obtain a single value.

The resulting uncertainty in the total pressure ratio (PR), corrected mass flow rate ($\dot{m}$) and isentropic total-to-total efficiency (η_{TT}) measurements are detailed in Table 2. For the purposes of presenting the data in the clearest possible fashion, only the extremities of the operating range for C-4 have been presented. C-4 was chosen as it represents the geometry with the largest operating speed range, and it is the smallest compressor meaning any uncertainty in the data acquisition procedure would have the most significant impact on the results.

Table 2: Experimental Uncertainty for C-4

Operating Point		PR (%)	η_{TT} (%)	$\dot{m}$ (%)
33% speed, surge point	Upper	+0.08	+1.37	+0.60
	Lower	-0.08	-1.32	-0.62
33% speed, choke point	Upper	+0.08	+1.50	+0.60
	Lower	-0.08	-1.41	-0.62
100% speed, surge point	Upper	+0.08	+0.35	+0.64
	Lower	-0.08	-0.35	-0.65
100% speed, choke point	Upper	+0.08	+0.32	+0.63
	Lower	-0.08	-0.32	-0.64

In order to minimise the impact of heat transfer on the measured efficiency values obtained from the test rig, steps were taken to control the levels of both internal and external heat transfer to and from the turbocharger. It is well known that in traditional hot gas stand testing, where turbine inlet temperatures representative of on-engine operation are utilised, underestimations of compressor efficiency at low tip speeds and flow rates of 20% can be witnessed [13]. With the current data set, a rigorous procedure of thermal matching across the turbocharger was employed at all points to control internal heat transfer levels, while fiberglass mat was wrapped around each turbocharger to control external heat transfer. The results of these efforts yielded a maximum deviation from calculated adiabatic conditions (in accordance with the method of Sirakov and Casey [14]) of just 2.1% for the smallest compressor geometry at minimum mass flow rate operating conditions, as illustrated in Figure 3. Further

detail on the testing procedure and heat transfer control methodology employed is provided in [3].

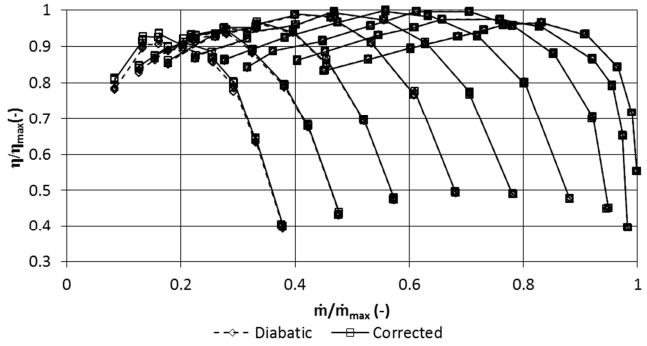

Figure 3: Comparison of diabatic and corrected efficiency test data for C-4

It is worth emphasizing that the CFD results presented have been post processed to include 1-D loss correlations for the volute and disk friction, as detailed in a previous section. The resulting comparisons between the single passage CFD results and test data are presented in Figure 4 to Figure 6 for C-4 to C-6 respectively.

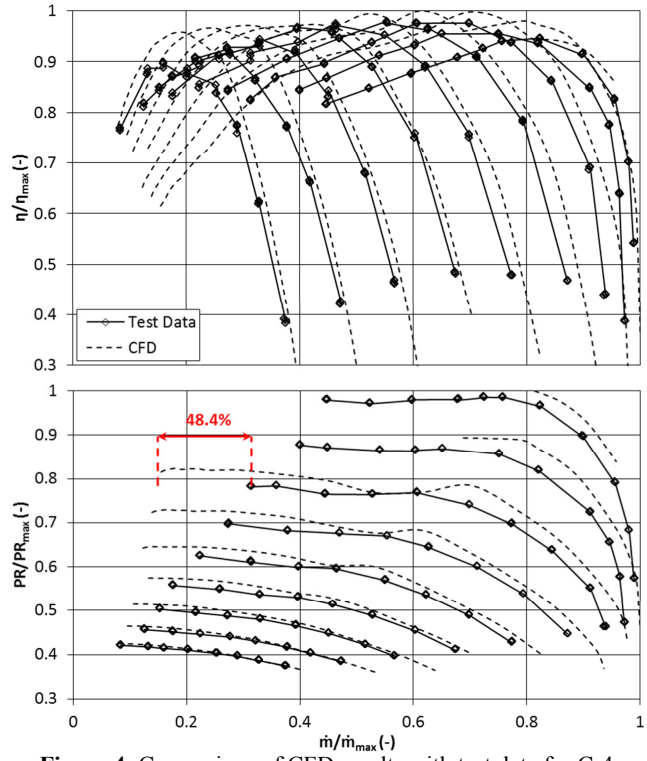

Figure 4: Comparison of CFD results with test data for C-4

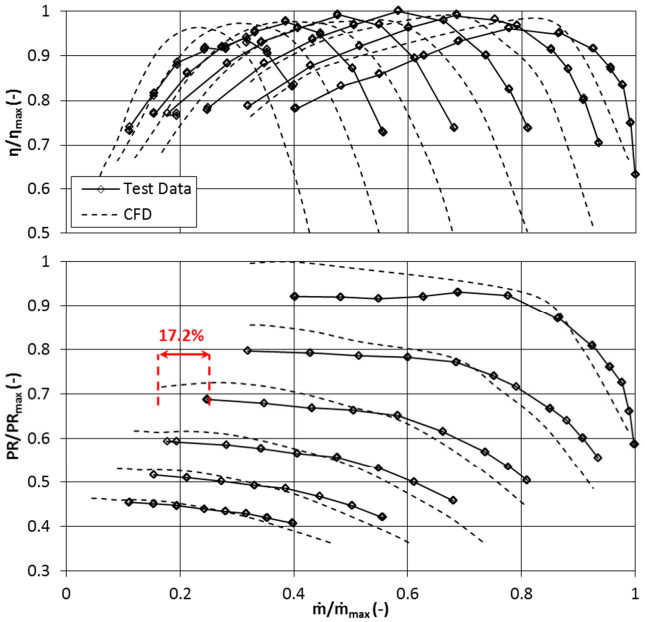

Figure 5: Comparison of CFD results with test data for C-5

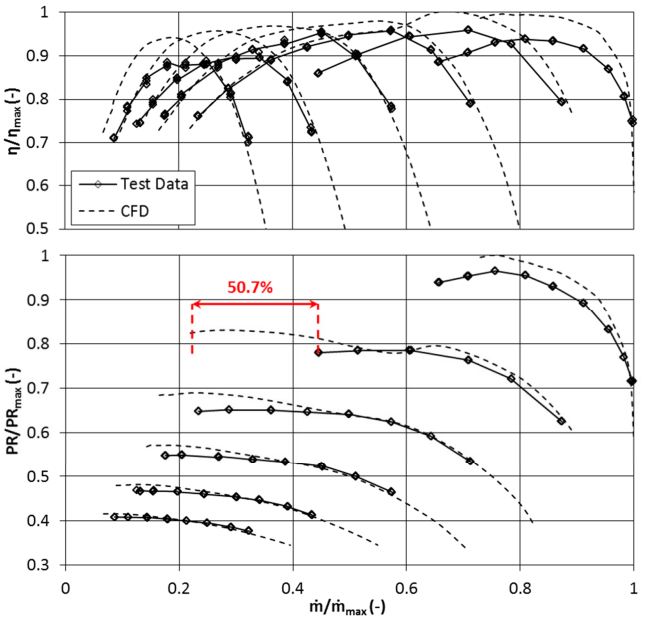

Figure 6: Comparison of CFD results with test data for C-6

Upon inspecting the results depicted in Figure 4 to Figure 6, it is apparent that the CFD has predicted performance within an acceptable window of accuracy. The pressure ratio and efficiency predictions follow the trend of the test data well, with the maximum variation between the data sets being witnessed at low mass flow rates for each of the compressors. It was demonstrated in a previous section that the test data is essentially devoid of the effects of heat transfer, however what little impact it did have on efficiency would be most prevalent at low speeds and low mass flows. It is notable that surge is frequently predicted at an unrealistically low mass flow rate when compared with the test data, with maximum deviations of 48.4%, 17.2% and 50.7% being witnessed for C-4 to C-6 respectively. It is of course recognised however that surge is a system phenomenon that is also fundamentally unsteady; the CFD model used did not represent the full system and assumed steady flow since surge prediction was not a primary target of the modelling work. In addition, for C-4 there were convergence issues which could not be resolved within the upper two speed lines, yielding a substantially truncated

map prediction at these operating conditions. These discrepancies are not entirely unexpected with a single passage simulation however. While a 1-D volute loss model has been applied, it is not sufficient to capture the non-axisymmetric, three-dimensional and unsteady nature of the volute flow field, and its impact on the performance and stability of components upstream at off-design conditions [15].

It must be noted that for C-4 specifically, there was an audible rotating stall / mild surge phenomenon taking place for a large portion of the maximum speedline during the testing procedure. While the testing could continue to take place down to much lower flow rates than was achieved for the CFD without invoking deep surge, it would appear that the instabilities induced made it impossible for convergence to be achieved for the steady state CFD simulation employed. Further validation of the presence of time varying flow phenomena was present in the RMS residual plots from the CFD for these points, where a sinusoidal variation was present, which is indicative of unsteady effects.

In fact, the prediction of surge to be at differing flow rates to the test data does not pose a problem for the current work. The blockage values used in a subsequent section, which represent the full extent for which CFD was used in the current work, were only extracted at mass flow rates that fall within the bounds of the operating range as defined by the test data. Therefore, with the magnitude of the CFD predictions having been shown to be reasonable within the confines of the test data, the methodology applied is fully sufficient for the current study.

CHARACTERISATION OF DIFFUSER BLOCKAGE

Having gained confidence in the accuracy of the CFD simulations, it was possible to move forward with the 1-D modelling work. In order to evaluate the radial extent of this aerodynamic blockage, the same approach was applied as was used in the diffuser inlet blockage study referred to in a previous section, but instead of being evaluated exclusively at diffuser inlet, it was applied at approximately 25 discrete radial locations from the inlet to exit of the diffuser (depending on geometry). Again, the Turbo Chart feature of ANSYS CFX was utilized to extract circumferentially averaged streamwise velocity and density values at 250 discrete points equally spaced from hub to shroud at each of the chosen streamwise locations for each compressor. Using the continuity equation, it was then possible to calculate the mass flow passing through each pitchwise "slice" of the diffuser passage (denoted "*dz*" in Figure 7). The extent of the active flow region was then calculated by summing from hub to shroud until the stage mass flow rate was reached. The proportion of the remaining diffuser slices in relation to the total number of 250 defined the extent of the aerodynamic blockage. A schematic representing this procedure is depicted in Figure 7.

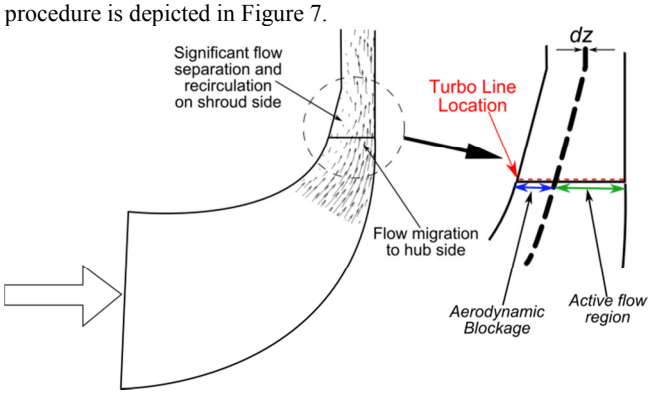

Figure 7: Determination of diffuser aerodynamic blockage

The result of this analysis is a diffuser passage that is defined by two separate regions; an active flow region through which the entirety of the stage mass flow is assumed to pass, and a blockage region which makes no contribution to outlet flow conditions. In effect, the approach is analogous to the use of boundary layer displacement thickness, where as far as the flow is concerned the passage area associated with the aerodynamic blockage is effectively not available for flow, and flow in the active flow region is treated with a single velocity value representative of the flow field at any given radius. The aerodynamic blockage region influences the flow field in three ways:

- increased radial velocity component V_{R2} (by continuity)
- reduction in absolute flow angle α_2
- modification of effective diffuser inlet to outlet area ratio

The first two parameters directly impact upon the flow field, while the final one has an indirect impact on actual diffuser performance through modifying the ideal achievable CP for the diffuser [16], as illustrated in Eq. (3). As will become apparent in the coming sections, this final element has a significant impact on diffuser performance.

$$CP_I = cos^2(\alpha_2)\left(1-\frac{1}{AR^2}\right) + sin^2(\alpha_2)\left(1-\frac{1}{RR^2}\right) \quad (3)$$

In order to capture the variation of blockage across the different geometries and operating conditions being tested, it was deemed necessary to formulate a simplified method reliant on data from only a number of operating points, rather than the full compressor map. The variation of the blockage throughout the diffuser was extracted at surge, choke and peak efficiency for all three geometries at a number of operating conditions. A sample result from this analysis is presented in Figure 8 for C-6 at 75% speed, detailing the CFD results as well as the correlations generated to replicate the blockage variation on a 1-D basis.

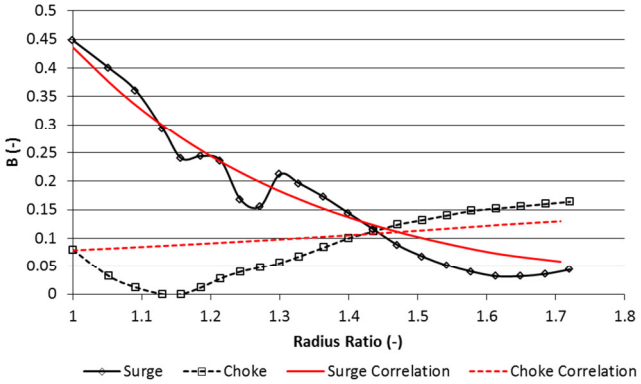

Figure 8: Diffuser blockage variation for C-6 at 75% speed

The trend illustrated in Figure 8 is one that was echoed across all three geometries at a range of operating conditions; the high levels of inlet blockage at surge depicted a tendency to decrease through the diffuser, while the comparatively low levels of inlet blockage at choke tended to increase with radius in the diffuser. At the surge side of the map, low velocity fluid is subject to a strong adverse pressure gradient, aggravating the tendency for boundary layer separation and recirculation. The relationship between blockage and diffuser radius ratio witnessed in Figure 8 can be attributed to the decay of this recirculation zone present close to impeller exit, as depicted in Figure 7. Towards choke, the fluid velocity is greater and the adverse pressure gradient much less severe. As a result, the recirculation region which is dominant at surge is no longer present, meaning the blockage presented to the flow is predominantly attributable to boundary layer growth from inlet to outlet of the diffuser. Therefore, having analysed the blockage levels throughout the diffuser for the three geometries under consideration at a range of operating conditions, it became apparent that the overall trend could be well represented (albeit on

a simplified basis) at both surge and choke by exponential functions, as illustrated in Figure 8.

The proposed correlations, as illustrated in Eq. (4) and (5), represent either an exponential decay or growth of the diffuser aerodynamic blockage for surge and choke respectively. The exponent "*x*" represents radial location in the diffuser, which equates to the quotient of the current calculation step, *i,* and the total number of calculation steps. Throughout the current analysis performance was evaluated using 100 radial steps through the diffuser, a value that was deemed to balance the competing aims of calculation time and prediction accuracy.

$$B_{i,surge} = B_2 e^{-2x} \tag{4}$$

$$B_{i,choke} = B_2 e^{0.5x} \tag{5}$$

At this stage, representative correlations have been generated for surge and choke, however no consideration has been given for mid map conditions. In order to accurately represent the blockage present away from the extremities of map width, a linear interpolation procedure was employed on the basis of the diffuser inlet flow angle α_2, as depicted in Eq. (6). This approach provided a smooth transition between the two correlations and, as will become apparent in the coming sections, a good estimation of diffuser performance across the operating range without the need for extensive knowledge about the flow field at every radial location in the diffuser at each operating point.

$$\begin{aligned} B_i &= B_{i,surge} + (B_{i,choke} \\ &\quad - B_{i,surge})\left(\frac{\alpha_2 - \alpha_{2,surge}}{\alpha_{2,choke} - \alpha_{2,surge}}\right) \end{aligned} \tag{6}$$

1-D DIFFUSER MODELLING

Based on the findings from the previous study [3], it was deemed that the most appropriate model to build upon for the current work was a model based upon an equation first presented by Rodgers [17], but subsequently converted into a vaneless diffuser modelling method by Stuart *et al.* [3]. The Rodgers equation permitted evaluation of diffuser CP directly, knowing only the overall diffuser geometry and inlet flow angle. This was further developed to calculate diffuser pressure recovery for each radial step, as well as the associated key flow parameters using a compressible analysis.

The reasoning behind this was that, ultimately, the aim was to develop a vaneless diffuser model for which each of the individual sources of loss were accounted for, and with the simplistic method outlined above only currently accounting for the impact of wall friction, it was deemed a good basis to build upon. In order to evaluate the improvement in prediction over existing methods, the Herbert model [6], which is an extension and correction of Stanitz' [5] ground breaking work, was chosen as it represented the most complex of the existing approaches, incorporating terms for boundary layer growth and total pressure loss as a function of Mach number and boundary layer shape factor.

Fundamentally, the proposed model evaluates the coefficient of static pressure rise, CP, for each calculation step in the diffuser, based upon geometry and a chosen value of skin friction coefficient C_f using the aforementioned Rodgers equation [17], as depicted in Eq. (7). Unlike a number of existing approaches which effectively employ the skin friction coefficient as a bulk loss term, it is intended that the variable in the proposed model accounts only for wall friction loss.

$$CP = \left[1 - \left(\frac{D_{(i)}}{D_{(i+1)}}\right)^2\right] - \frac{C_f}{\cos(\alpha_i)}\frac{D_{(i)}}{b_{(i)}}\left(1 - \frac{D_{(i)}}{D_{(i+1)}}\right) \tag{7}$$

From this, the ideal isentropic coefficient of static pressure rise, CP_I, is evaluated using Eq. (3), and compared with the actual value calculated using Eq. (7) to allow the vaneless diffuser loss coefficient Y_D to be calculated, as shown in Eq. (8).

$$Y_D = CP_I - CP \tag{8}$$

Knowing the value of Y_D, it is possible to calculate the change in total pressure across the current calculation step, and hence evaluate the total pressure applicable to the following step, as illustrated in Eq. (9) and Eq. (10) respectively.

$$dp_o = Y_D\left(p_{o(i)} - p_{(i)}\right) \tag{9}$$

$$p_{o(i+1)} = p_{o(i)} - dp_o \tag{10}$$

Before moving on to calculate the remaining flow variables, it is necessary to incorporate the impact of the previously described aerodynamic blockage on the flow field. In order to incorporate the blockage correlations into a 1-D modelling method, the direct impact on the flow field had to be evaluated. The first parameters requiring evaluation for each calculation step were the diffuser inlet flow parameter ϟ, and the associated quartic relationship for diffuser inlet blockage B_2, as depicted in Eq. (1) and (2) respectively. Knowing these parameters, and the exponent *x*, it is possible to evaluate the surge and choke blockage relationships given by Eq. (4) and (5), and ultimately calculate the blockage at any step using the linear interpolation based on absolute diffuser inlet flow angle α_2 detailed in Eq. (6).

Knowing the blockage presented to the flow, it was possible to evaluate the direct impact on the radial velocity using the continuity equation, as illustrated in Eq. (11).

$$V_{ri} = \frac{\dot{m}}{\rho_i(1 - B_i)(2\pi r_i b_i)} \tag{11}$$

As the analysis is compressible in nature, a further internal iterative process was incorporated into the analysis to determine the density at each step. This involved undertaking the above procedure, then continuing the calculation to determine the total and static pressure and temperature values associated with the newly calculated flow conditions. From the resulting static pressure and temperature values, a new density was calculated using the equation of state (as depicted in Eq. (12)), and compared with the initial value.

$$\rho_i = \frac{p_i}{RT_i} \tag{12}$$

If satisfactory convergence between the two density values was not achieved, the entire calculation was completed again, beginning with the determination of the blockage level, until such a point where the solution was deemed to have converged.

Having specified the basis of the proposed modelling method, it was possible to evaluate its impact on the prediction of diffuser performance. The parameter upon which the modelling methods will be evaluated is the coefficient of static pressure rise (CP). CP, as depicted in Eq. (13), captures the fundamental purpose of a centrifugal compressor diffuser, by providing a metric to determine the proportion of total pressure at inlet of the diffuser that was successfully converted into static pressure at the exit of the diffuser.

$$CP = \frac{p_3 - p_2}{p_{02} - p_2} \tag{13}$$

As a first step, a direct comparison of diffuser CP prediction was undertaken for each of the geometries. This utilised the same methodology as was applied by Stuart *et al.* [3], where diffuser inlet conditions were specified entirely from testing data to ensure the integrity of the comparison and to remove any discrepancies attributed to limitations in the meanline impeller modelling. The resulting comparison between test data, the Herbert model and the proposed model for each of the three geometries is presented in Figure 9.

In order to improve the clarity of the resulting comparison, only three speedlines (representing low, medium and high tip speeds) for each geometry are presented. Furthermore, the values of CP in each case have been non-dimensionalised using the maximum value of CP achieved across all three geometries, be that from test results or 1-D predictions. It must be noted that this approach is in contravention of what was conducted for the other figures within the manuscript, where the maximum value for a given parameter was taken for each compressor individually. However, it helps to illustrate a key observation within the discussion that follows.

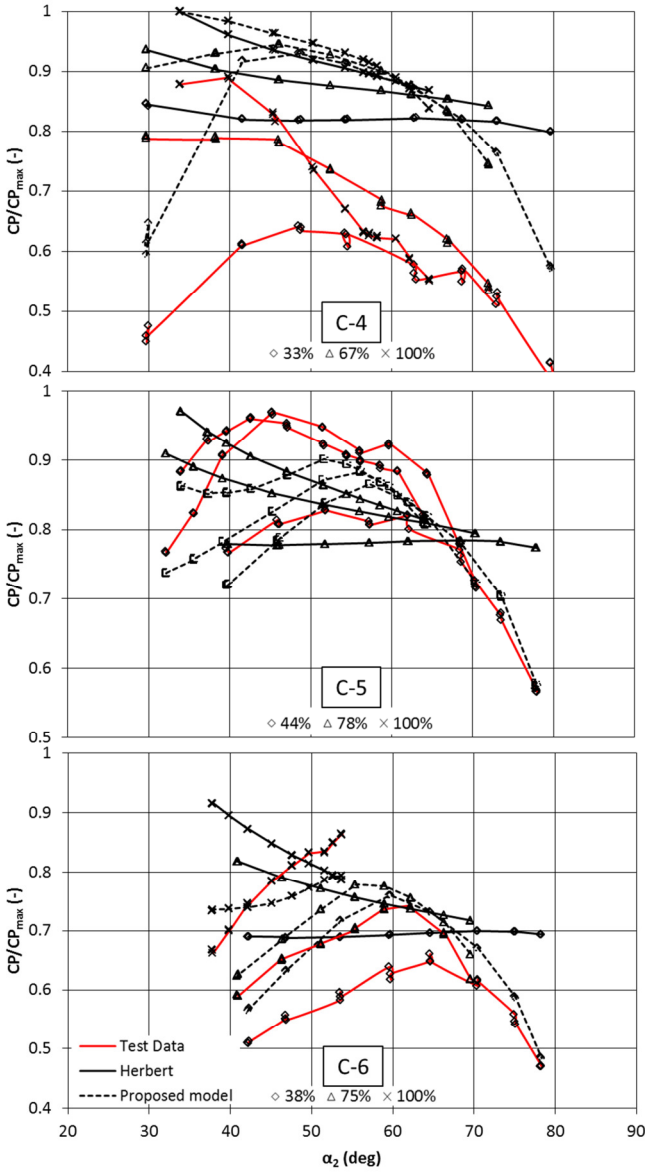

Figure 9:1-D diffuser modelling comparison

Discussion

What is immediately apparent from analysing Figure 9 is that the baseline Herbert model is lacking the ability to predict the trend of how CP varies with α_2 across the compressor map. Despite the relative complexity of the modelling method as explained in the preceding sections, the predominant feature of the approach is the impact of the skin friction coefficient C_f. This dictates that CP variation across the map will be mainly reliant on the relationship between the chosen friction coefficient, and the flow path length within the diffuser. As a result, for a given value of C_f, CP will be maximum for the lowest value of α_2, which corresponds to the shortest flow path, and consistently decrease as the flow angle becomes more tangential. Due to the additional parameters in the model relating the loss in total pressure through the diffuser to the boundary layer shape factor, which in turn is dependent upon Mach number, there is some spreading of the speedlines at a constant value of α_2. However, even with this addition the influence of the friction loss is still predominant.

A further point worth noting is that it is evident that, generally speaking, the 1-D modelling methods deliver better correlation with the test data for C-5 and C-6 than for C-4, which has the smallest impeller but the largest diffuser radius ratio of the three test cases. It is readily apparent from Figure 9 therefore that the increase in the ideal CP, as depicted in Eq. (3), brought about by the larger radius ratio (RR) of C-4 is not sufficiently counteracted by the increased frictional losses associated with the longer flow path for a given increase in flow angle within the diffuser.

With respect to the proposed modelling method, it is clear that it offers an improved prediction, particularly at the extremes of the compressor operating map. At higher values of α_2 the approach of directly applying the loss in total pressure associated with the skin friction coefficient in each geometry step delivers a more accurate representation of real performance when compared with the Herbert model, illustrated by the substantial performance decrement towards surge. For example, considering the maximum α_2 values reached by C-5 for each of the three speedlines under consideration, the maximum deviation from the test data witnessed with the proposed model was 1.0% compared with 25.7% for the Herbert model. Similarly, for C-6 the largest discrepancy with the test data witnessed was 13.6% compared to a value of 43.6% with the Herbert model. As described above, the correlation achieved for C-4 was not as impressive as for the other two geometries, however the proposed method still delivers a more representative prediction than that achieved by the Herbert model.

At the opposite side of the performance map, the performance decrement towards choke that is evident in the test data, which is absent in the Herbert prediction, is captured well by the proposed model, especially for C-5 and C-6. Comparing again the maximum deviation between the test data and each of the modelling methods, this time at minimum α_2, for C-5 this amounted to 7.0% for the proposed model, compared to 22.2% for the Herbert model. Similarly, for C-6 the maximum deviation of 12.9% for the proposed model compares favourably with the 48.6% arising from the Herbert model. In the same vein as previously mentioned, the prediction from the proposed method for C-4 did not follow as well as for the other two geometries, but still offered an improvement over the baseline Herbert method. While the reasoning behind this has been covered in the preceding paragraphs, further work would be required to gain an understanding of the best way to modify the model to account for the difference in performance for C-4.

In terms of an explanation for the drop off in performance towards choke (low values of α_2) within the proposed model, the blockage correlation for choke as depicted in Eq. (5) dictates that from inlet to outlet, the level of blockage presented to the flow must increase. As a result, the effective geometry of the diffuser has been modified, meaning the area increase associated with each

calculation step is much less than would be expected taking only the physical geometry into account.

It is clear therefore that while the levels of blockage at the inlet of the diffuser are much smaller at choke than at surge, it is the growth of the blocked region towards choke that causes the significant decrement in performance. As the effective passage height is reducing for each calculation step, the area increase associated with the increase in radius is diminished over the case with no blockage, or the surge case. Going back to Eq. (3), the reduction in the area ratio of the diffuser brings about a reduction in the ideal achievable CP, resulting in the ability to replicate the performance decrement witnessed in the test data. It is clear therefore from the current model that wall friction is still the predominant 1-D source of loss towards surge, but aerodynamic blockage throughout the diffuser has been identified to be a significant contributing factor towards the choke side of the map.

IMPACT ON 1-D STAGE CALCULATION

As a final verification of the benefit of the proposed vaneless diffuser model, the decision was taken to evaluate the impact on a 1-D stage performance prediction, incorporating models for the impeller, vaneless diffuser and volute. The impeller losses applied to the model originated from the work of Galvas [18], with the inlet recirculation model of Harley *et al.* [1], the choking loss of Aungier [19] and the clearance loss of Jansen [20] also applied. The slip factor correlation applied was that of Qiu *et al.* [21], with the volute loss again being accounted for using the work of Weber and Koronowski [9]. As with the previous section detailing a diffuser only performance evaluation, the vaneless diffuser model used for comparison against the proposed model was that of Herbert [6].

The resulting comparisons for C-4 to C-6 are illustrated in Figure 10 to Figure 12 respectively, where all data have been normalised using the maximum respective value for that parameter. As with the previous section, to preserve the clarity of the comparison only three speed lines per geometry have been presented, representing low, medium and high tip speed operation.

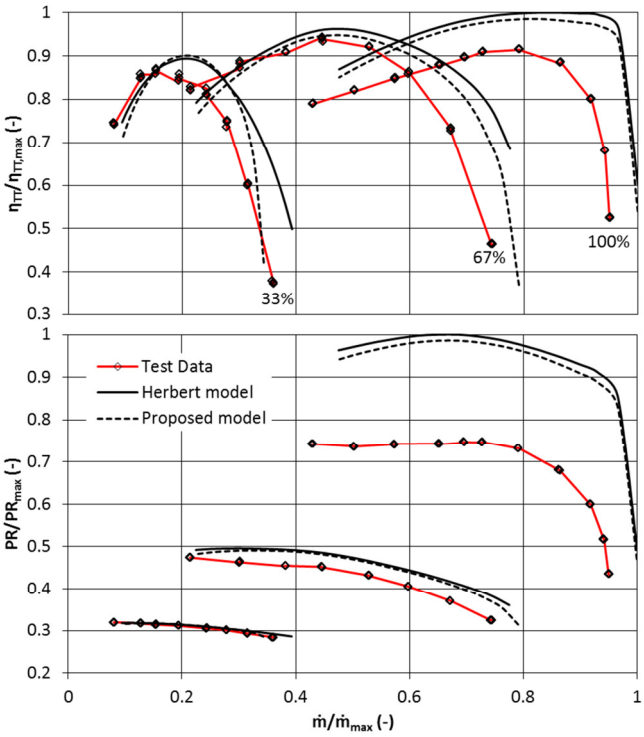

Figure 10: Comparison of 1-D modelling with test data for C-4

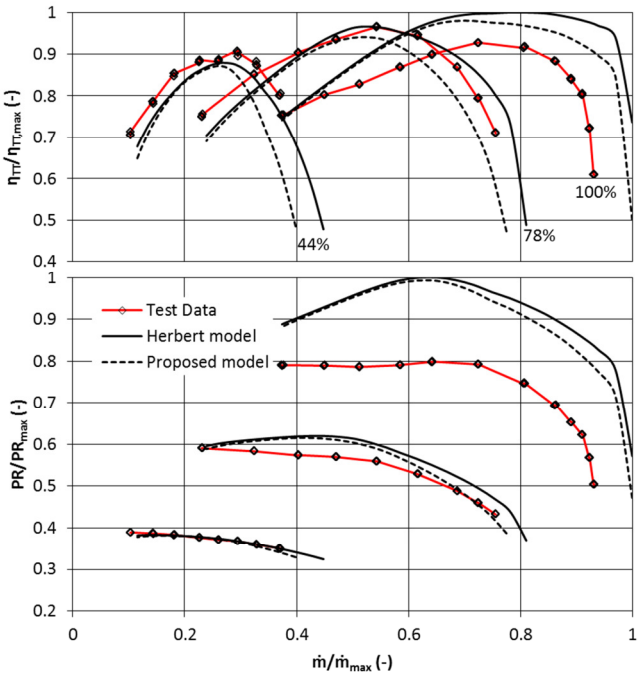

Figure 11: Comparison of 1-D modelling with test data for C-5

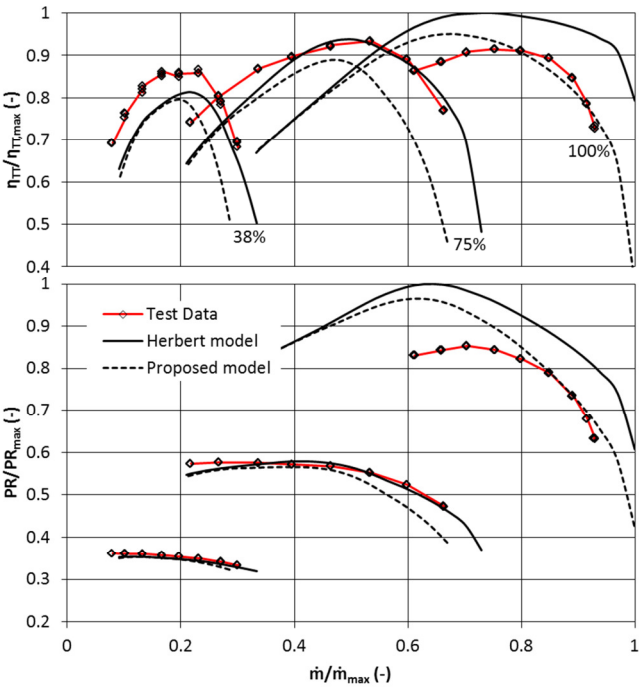

Figure 12: Comparison of 1-D modelling with test data for C-6

Discussion

What is instantly striking about the comparisons illustrated in Figure 10 to Figure 12 is that the magnitude of the improvement in the prediction achieved on a diffuser only basis has not been reflected as significantly on a stage performance basis. Generally speaking, the change in performance associated with the proposed model has a greater impact on the choke side of the map, however while this is advantageous in bringing the prediction closer to the test data at higher speeds, it generally has a detrimental impact on the lower speed lines. This observation is particularly pertinent for C-6, as depicted in Figure 12.

A common observation for each of the geometries is that the accuracy of both the pressure ratio and efficiency predictions diverge as compressor speed increases. The trend depicted in the test data concerning the drop in peak compressor efficiency at high speeds is one that is not captured by the existing 1-D

modelling technique, resulting in diminishing efficiency prediction with increasing speed. As noted by Harley *et al.* [1], this trend is common in automotive turbocharger compressors, where designs are specifically targeting improved efficiency at low speeds and mass flow rates to better align with the engine transients encountered during urban driving.

What is also evident is while the efficiency prediction diverges at higher speeds, the prediction of pressure ratio does so at an increased rate. Taking C-5 as an example, on the 100% speedline at $\dot{m}/\dot{m}_{max}$ of 0.75, the error in the efficiency prediction equates to 5.6% between the test data and proposed model, while the pressure ratio prediction illustrated an associated error of 21.3%. Upon investigating this problem more deeply, it became apparent that the discrepancy was related to the prediction of the tangential velocity at impeller exit (V_{u2}) from the single zone model. Comparing the prediction of V_{u2} from the single zone model to that from the previously described CFD simulations, an over prediction of 19.2% by the single zone model was evident for the same operating point for C-5. It would appear that the issue here relates to the determination of the impeller slip factor, as if it was over predicted, it would manifest itself as an increase in predicted pressure ratio (in accordance with the Euler equation). However, as slip factor is not a loss, it would not have the same impact on efficiency, which is exactly the symptom depicted in the current data set. Therefore, despite the rigour with which the slip factor correlation of Qiu *et al.* [2] was derived, it is possible that further work would be required to better match the current data set.

A further issue with the 1-D prediction is the prediction of the choking mass flow rate, the accuracy of which again diverges with increasing compressor speed. The current method applied is that of Dixon & Hall [22], which compares the available inducer throat geometric area to a calculated choking area based on total inlet conditions. Unfortunately, this simplified approach cannot account for the highly non-uniform velocity profile at the throat section and the associated boundary layer blockage [23], which like in the current work, results in the full geometric area not being available to pass the stage mass flow. Consequently, choking in the real stage occurs significantly earlier than what is predicted by the simplistic 1-D analysis currently applied. Again, further work is required to improve the fidelity of the choking model to account for these real flow effects.

CONCLUSIONS

Improvements in the 1-D prediction of vaneless diffuser performance have been achieved through the analysis of three automotive turbocharger centrifugal compressor stages. A combination of extensive gas stand test data, which was shown to have been gathered under approximately adiabatic conditions, as well as single passage CFD simulations for each geometry were employed to permit full characterisation of the diffuser flow field.

Modelling of the extent of the aerodynamic blockage presented to the flow throughout the diffuser with changing geometry and operating conditions was completed on a simplified basis, and was illustrated to have a significant impact on diffuser performance. Correlations describing the variation in the aerodynamic blockage throughout the diffuser resulting from the stratified flow field emanating from the impeller were developed, and incorporated into a new diffuser modelling method described herein.

Utilising the methodology developed by the authors for a previous study, direct comparisons were drawn between the diffuser performance prediction delivered by the proposed model, the baseline 1-D Herbert model and test data. By providing the 1-D models and test data with effectively common input parameters, a robust diffuser-only performance analysis was conducted for each of the geometries, validating significant improvements in the off-design performance prediction delivered by the proposed model. This improved performance prediction for vaneless diffusers is certainly beneficial at the preliminary design stage, allowing the designer to consider appropriate geometry before committing to 3-D CFD modelling.

Upon incorporating the proposed diffuser model into a 1-D stage calculation, the limitations in the modelling of the other stage elements (particularly the impeller) masked the benefits witnessed on a diffuser-only basis. Comparing the 1-D stage prediction with test data for each geometry did however provide some guidance for future work, with the divergence in pressure ratio and efficiency prediction towards higher speeds and the overall choking mass flow prediction providing focal points.

ACKNOWLEDGEMENTS

The authors would like to sincerely thank IHI Charging Systems International GmbH for provision of the necessary compressor hardware for testing, as well as for their continuing technical support. The authors would also like to extend their thanks to ANSYS Inc. for the use of their CFD software and their technical support during this programme of research.

REFERENCES

[1] Harley, P., Spence, SW., Filsinger, D., Dietrich, M., & Early, J., 2015, "Meanline Modeling of Inlet Recirculation in Automotive Turbocharger Centrifugal Compressors," *ASME Journal of Turbomachinery*,Vol.137 (1)

[2] Qiu, X., Japikse, D., & Anderson, M., 2008, "A Meanline Model for Impeller Flow Recirculation," Proceedings of *ASME Turbo Expo 2008*, Berlin, Germany, GT2008-51349

[3] Stuart, C., Spence, S.W., Filsinger, D., Starke, A., Kim, S., & Harley, P., 2015, "An Evaluation of Vaneless Diffuser Modelling Methods as a Means of Improving the Off-Design Performance Prediction of Centrifugal Compressors," *Proceedings of ASME Turbo Expo 2015*, Montréal, Canada, GT2015-42657

[4] Cumpsty, N.A., 2004, "*Compressor Aerodynamics*," Krieger Publishing Company, Florida, ISBN 1-57524-247-8, pp277

[5] Stanitz, J.D., 1952, "One-dimensional compressible flow in vaneless diffusers of radial- and mixed-flow centrifugal compressors, including the effects of friction, heat transfer and area change," *National Advisory Committee for Aeronautics*, Technical Note 2610, Washington, USA

[6] Herbert, M.V., 1980, "A Method of Performance Prediction for Centrifugal Compressors," *ARC R&M No. 3843*, H.M. Stationery Office, London, England

[7] Dubitsky, O., & Japikse, D., 2008, "Vaneless Diffuser Advanced Model," *ASME Journal of Turbomachinery*, Vol. 130 (1)

[8] Stern, F., Wilson, R.V., Coleman, E.W., & Paterson, E.G., 2001, "Comprehensive Approach to Verification and Validation of CFD Simulations – Part 1: Methodology and Procedures," *ASME Journal of Fluids Engineering*, Vol. 123 (4)

[9] Weber, C.R., & Koronowski, M.E., 1986, "Meanline Performance Prediction of Volutes in Centrifugal Compressors," *Proceedings of ASME Turbo Expo*, Dusseldorf, Germany, 86-GT-216

[10] Whitfield, A., 1974, "Slip Factor of a Centrifugal Compressor and its Variation with Flow Rate," *Proc Instn Mech Engrs* Vol. 188 32/74 pp415-421

[11] SAE J1826, March 1995, "Turbocharger Gas Stand Test Code," *Society of Automotive Engineers*, Pennsylvania, USA

[12] British Standards Institution, 1984, "BS1904: Specification for industrial platinum resistance thermometer sensors", *British Standards Institution,* London, UK

[13] Baines, N., Wygant, K.D., & Dris, A., 2011, "The Analysis of Heat Transfer in Automotive Turbochargers," *ASME Journal of Engineering for Gas Turbines and Power*, Vol. 132

[14] Sirakov, B., & Casey, M., 2011, "Evaluation of Heat Transfer Effects on Turbocharger Performance," Proceedings of *ASME Turbo Expo 2011*, Vancouver, Canada, GT2011-45887

[15] Yang , M., Zheng, X., Zhang, Y., Bamba, T., Tamaki, H., Huenteler, J., & Li, Z., 2010, "Stability Improvement of High-Pressure-Ratio Turbocharger Compressor by Asymmetric flow Control: Part I-Non Axisymmetric flow in Centrifugal Compressor," *Proceedings of ASME Turbo Expo 2010*, Glasgow, Scotland, GT2010-22581

[16] Whitfield, A., & Baines, N.C., 1990, "*Design of Radial Turbomachinery*," Longman Scientific & Technical, Essex, England, pp118

[17] Rodgers, C., 1984, "Static pressure recovery characteristics of some radial vaneless diffusers," *Canadian Aeronautics and Space Journal*, Vol. 30, Issue, 1, pp42-54

[18] Galvas, M. R., 1974, "Fortran Program for Predicting Off-Design Performance of Centrifugal Compressors," *NASA Lewis Research Center*, Cleveland, OH, Paper No. NASA-TN-D-7487.

[19] Aungier, R. H., 2000, "*Centrifugal Compressors: A Strategy for Aerodynamic Design and Analysis"*, ASME Press, New York.

[20] Jansen, W., 1967, "A method for calculating the flow in a centrifugal impeller when entropy gradients are present," *University of Cambridge Internal Aerodynamics (Turbomachinery) Conference, UK*

[21] Qiu, X., Mallikarachchi, C., and Anderson, M., 2007, "A New Slip Factor for Axial and Radial Impellers," *Proceedings of ASME Turbo Expo 2007*, Montréal, Canada, GT2007-27064

[22] Dixon, S.L., & Hall, C.A., 2010, "*Fluid Mechanics and Thermodynamics of Turbomachinery*," Butterworth-Heinemann, USA, pg 256-258

[23] Van den Braembussche, R,A,, 2014, "Centrifugal Compressors Analysis & Design," *VKI Course Note 192*, pg 72